Journal of New Materials for Electrochemical Systems 15, 83-88 (2012)

Development of Inorganic-organic Membranes Consisting of $ZrO_2 \cdot nH_2O$ and Sulfonated-PES for Direct Methanol Fuel Cells

Takayuki Hirashige, Tomoichi Kamo, Takao Ishikawa and Takeyuki Itabashi

Central Research Laboratory, Hitachi Ltd., Akanuma 2520,
Hatoyama-machi, Hiki-gun, Saitama, 350-0395, Japan

Received: November 08, 2011, Accepted: December 08, 2011, Available online: January 27, 2012

Abstract: *We investigated inorganic-organic membranes consisting of sulfonated-poly(ether sulfone) (S-PES) and $ZrO_2 \cdot nH_2O$ with the aim of improving proton conductivity and blocking methanol. We prepared excellent uniform membranes by the method using $ZrOCl_2 8H_2O$ as a precursor. The proton conductivity of the $ZrO_2 \cdot nH_2O$/S-PES (EW=850) composite membrane with 50wt% $ZrO_2 \cdot nH_2O$ content was about four times higher than that of S-PES (EW=850). On the other hand, the methanol permeability of the $ZrO_2 \cdot nH_2O$/S-PES (EW=850) composite membrane with 50wt% $ZrO_2 \cdot nH_2O$ content was almost the same as that of S-PES (EW=850). These results mean in the composite membranes, the trade-off relationship between proton conductivity and methanol permeability found in S-PES was improved. The initial I-V performance of an MEA consisting of the $ZrO_2 \cdot nH_2O$/S-PES (EW=850) composite membrane with 50wt% $ZrO_2 \cdot nH_2O$ content showed a maximum power density of 65 mW cm^{-2} at 260 mA cm^{-2}.*

Keywords:

1.INTRODUCTION

Direct methanol fuel cells (DMFCs) have attracted considerable attention because they are promising candidates as power supplies for portable equipment. However, the low power density of DMFCs restricts their usage in many applications. It is necessary for further development of DMFCs to improve the power density of the membrane electrode assembly (MEA).

The membrane is the key component for improving the performance of MEA. There are two problems with the membrane. The first is low proton conductivity, which causes an increase in the IR-drop of the cell. Another problem is methanol permeability, namely methanol crossover, which causes an increase in the overpotential of the cathode, thus reducing power density. Moreover, it reduces the energy density of the DMFC because methanol permeability limits the methanol concentration. Thus, suitable membranes with high proton conductivity and low methanol permeability are required.

Two types of membranes are conventionally used in DMFCs. Perfluorosulfonic acid membranes such as Nafion, which have a cluster structure, are the most popular membranes for fuel cells [1-4]. They exhibit high proton conductivity because protons migrate through the cluster. But at the same time they exhibit high methanol permeability because methanol is also transported through the cluster. Hydrocarbon-based membranes, on the other hand, have little or no cluster structure [5- 8]. In general, the methanol permeability of these membranes is lower than that of perfluorosulfonic acid membranes. However, the proton conductivity of these membranes is also low. In single polymer membranes, then, there is a trade-off relationship between proton conductivity and methanol permeability.

Recently, inorganic-organic membranes have attracted considerable attention, because they have the potential to mitigate the faults of single polymer membranes [9-19]. Both perfluorosulfonic acid membranes and hydrocarbon-based membranes have been used for organic component. For example, N. Miyake *et al.* prepared Nafion dispersing SiO_2 [9]. The membranes with 20wt% silica showed significantly lower methanol permeability. B. Libby *et al.* prepared polyvinylalcohol membranes containing mordenite

*To whom correspondence should be addressed: Email:
Phone:

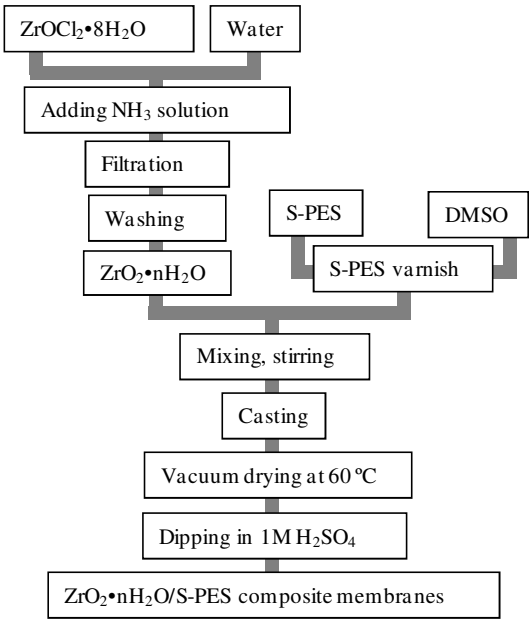

Figure 1. Preparation procedure of the simple dispersion method

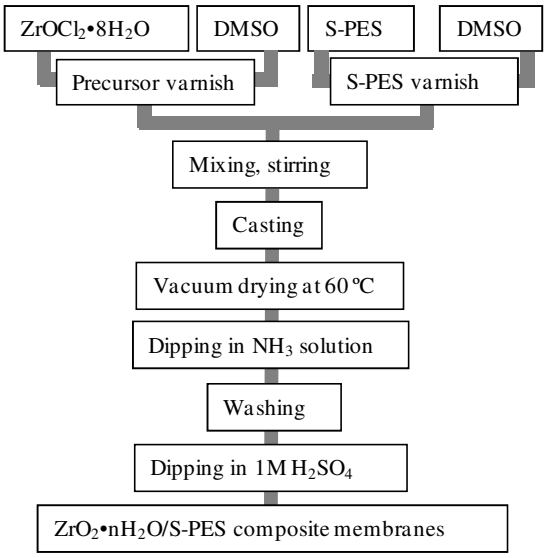

Figure 2. Preparation procedure of the precursor dispersion method

[10]. These membranes have twenty times better selectivity for protons over methanol than perfluorosulfonic acid membranes. T. Mitsui *et al.* prepared composite membranes consisting of three-dimensionally ordered macroporous silica and an ion exchange gel polymer [11]. These membranes prevent crossover of methanol due to a suppression of the polymer electrolyte swelling. Thus, inorganic-organic membranes are expected to realize both high proton conductivity and low methanol permeability.

On the other hand, it was difficult to obtain the inorganic-organic membranes with well-dispersed inorganic components, because inorganic components were easily aggregated.

In this work, we developed new preparation method for inorganic-organic membranes consisting of sulfonated-poly(ether sulfone) (S-PES) and well-dispersed metal oxide hydrate. We selected $ZrO_2{\cdot}nH_2O$ as the metal oxide hydrates. The proton conductivity of $ZrO_2{\cdot}nH_2O$ is higher than that of S-PES, and the protons are conducted through water in the crystal. Part of the water in the crystal is fixed as interlayer water and crystal water [20]. Methanol may be blocked by the metal oxide hydrate because methanol moves together with water. Thus, we distributed $ZrO_2{\cdot}nH_2O$ through the S-PES with the aim of improving proton conductivity and blocking methanol. The object of this paper is to develop a new synthetic scheme for $ZrO_2{\cdot}nH_2O$/S-PES composite membranes with high proton conductivity and low methanol permeability.

2.EXPERIMENTAL

2.1. Membrane preparation

We used two methods to prepare $ZrO_2{\cdot}nH_2O$/S-PES inorganic-organic composite membranes. The first was named the "simple dispersion method". In this method, $ZrO_2{\cdot}nH_2O$ powder was synthesized in advance. $ZrO_2{\cdot}nH_2O$ powder was mixed with S-PES varnish, then, cast to form the membrane film. Figure 1 shows a preparation procedure of the simple dispersion method. First, $ZrO_2{\cdot}nH_2O$ powder was synthesized from $ZrOCl_28H_2O$. $ZrOCl_28H_2O$ was dissolved in water, then, NH_3 solution was added to the solution. The $ZrO_2{\cdot}nH_2O$ was precipitated by hydrolysis as follows:

$$ZrOCl_2 + (n+1)H_2O \rightarrow ZrO_2{\cdot}nH_2O + 2H^+ + 2Cl^-$$

The $ZrO_2{\cdot}nH_2O$ powder was then filtered and washed with 1M KOH solution and distilled water several times to remove the chloride ion Cl^-. In parallel, S-PES was dissolved in dimethyl sulfoxide (DMSO). The obtained $ZrO_2{\cdot}nH_2O$ powder was mixed with the S-PES varnish, then, the varnish was cast with an applicator onto a glass plate to form the membrane film. The DMSO was evaporated under vacuum at 60 ℃. The membrane was dipped in 1M H_2SO_4. Thus, we prepared $ZrO_2{\cdot}nH_2O$/S-PES composite membranes.

Another method for preparing $ZrO_2{\cdot}nH_2O$/S-PES composite membranes was named the "precursor dispersion method". In this method, $ZrOCl_28H_2O$ was used as a precursor of $ZrO_2{\cdot}nH_2O$. Figure 2 shows a preparation procedure of the precursor dispersion method. Varnishes dissolving the S-PES and $ZrOCl_28H_2O$ respectively in DMSO were prepared and mixed together with a stirrer. Then, the mixed varnish was cast onto a glass plate using an applicator to form the membrane film. The DMSO was evaporated under vacuum at 60 ℃. Then, the film was dipped in 25wt% NH_3 solution to form $ZrO_2{\cdot}nH_2O$ by hydrolysis in the membrane. The membrane was washed in 1M KOH solution and distilled water several times to remove the chloride ion Cl^-. The membrane was dipped in 1M H_2SO_4. Thus, we prepared $ZrO_2{\cdot}nH_2O$/S-PES composite membranes.

The content of $ZrO_2{\cdot}nH_2O$ in the composite membranes varied from 0 to 60wt%. S-PES was prepared by modifying (using different monomers) the procedure reported in the literature [21]. S-PES with equivalent weights (EWs) of 752, 850, 1099, and 1347 was used for the base polymers. The thicknesses of the prepared membranes were 50 micrometer, respectively.

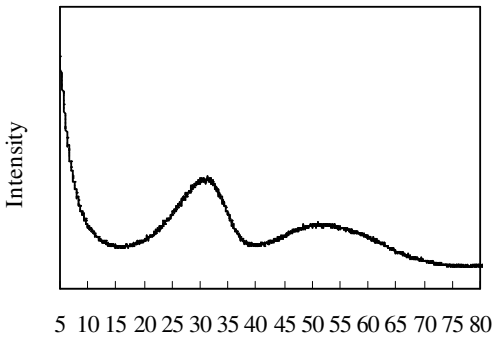

Figure 3. XRD pattern of $ZrO_2 \cdot nH_2O$ powder

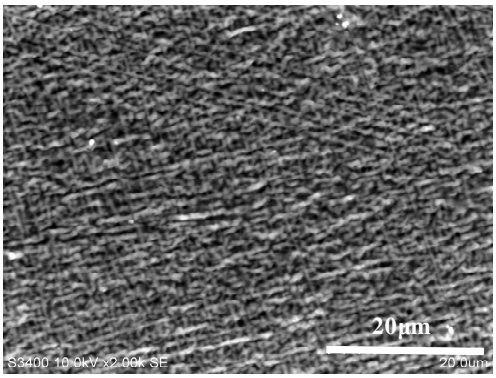

Figure 4. SEM image of the surface of the obtained membrane

2.2. MEA preparation

The MEA was fabricated by coating catalyst slurry directly to the membrane. The cathode catalyst slurry was prepared by mixing 5 wt% Nafion solution (Aldrich) and 50 wt% Pt/C (Tanaka Kikinzoku Kogyo), and the anode catalyst slurry was prepared by mixing 5 wt% Nafion solution and 54 wt% PtRu/C (Tanaka Kikinzoku Kogyo). Then, these catalyst slurries were coated directly on the membrane using a spray coater (Nordson). The catalyst loadings were 2.0 mg cm^{-2} for the cathode and 6.0 mg cm^{-2} for the anode. The geometrical electrode area of the MEA was 9.0 cm^2.

2.3. Proton conductivity measurements

The proton conductivity of the membranes was measured with a four-point probe method using LCR meter (Agilent Technologies 4284A). The membrane was fixed with two Teflon plates. The impedance between two platinum wires pressing on the membrane was measured using the LCR meter in a thermohygrostat at 70 ℃, 95 %RH.

2.4. Methanol permeability measurements

The methanol permeability of the membranes was measured using an electrochemical method, as proposed by X. Ren *et al.* [22]. The anode was filled with a 5wt% methanol solution, and the cathode was filled with N_2 gas. Methanol penetrates through the membrane from the anode to the cathode. The cell was loaded with a constant voltage using a potensio/galvanostat (Solartron 1480) and the current density was measured. The reactions were as follows: in the cathode catalyst layer, methanol was oxidized and protons and CO_2 were formed; in the anode catalyst layer, the proton was reduced and H_2 was formed. In these reactions, the rate-limiting factor is methanol permeability through the membrane. The steady-state limiting current density is determined by the flux rate of methanol permeability. So methanol permeability can be evaluated from the current density.

2.5. Characterization by microscopy

Crystallographic structure of $ZrO_2 \cdot nH_2O$ was analyzed using X-ray diffractometer (XRD) with Cu Kα radiation (Rigaku RU-200BH). Morphology of the obtained membrane was observed by using a scanning electron microscope (SEM) with an acceleration voltage of 10kV (Hitachi S3400). Dispersibility and particle size of the $ZrO_2 \cdot nH_2O$ in the composite membranes were observed by using transmission electron microscope (TEM) with an acceleration voltage of 200kV (Hitachi HF-2200).

2.6. Fuel cell performance evaluations

The I-V characteristic of the MEA consisting of the composite membrane with 50wt% $ZrO_2 \cdot nH_2O$ content was evaluated at room temperature using a potensio/galvanostat (Solartron 1480). A 20wt% methanol solution was fed to the anode for fuel at a speed of 6 ml min^{-1}. Air was supplied to the cathode with spontaneous flow.

The performance stability of the MEA was investigated by galvanostatic operation loading continually at 50 mA cm^{-2}. A 20wt% methanol solution was fed to the anode for fuel at a speed of 6 ml min^{-1}. Air was supplied to the cathode with spontaneous flow.

3. RESULTS AND DISCUSSION

3.1. Appearance of membranes

Figure 3 shows XRD pattern of $ZrO_2 \cdot nH_2O$ powder prepared by hydrolysis. There was no sharp peak, so $ZrO_2 \cdot nH_2O$ was rather an amorphous structure.

In the $ZrO_2 \cdot nH_2O$/S-PES composite membranes prepared by the simple dispersion method, white grains are aggregated. It is thought that these white grains are $ZrO_2 \cdot nH_2O$. This is attributed to the poor dispersibility of $ZrO_2 \cdot nH_2O$.

On the other hand, the appearance of $ZrO_2 \cdot nH_2O$/S-PES composite membranes prepared by the precursor dispersion method is uniform. Figure 4 shows SEM image of the surface of the obtained membrane with 50wt% $ZrO_2 \cdot nH_2O$ content. The membrane shows rough surface but no open pore. The distribution of $ZrO_2 \cdot nH_2O$ in the membrane was very homogenous.

The appearance varied with the $ZrO_2 \cdot nH_2O$ content: the membranes were transparent for 10wt%, translucent for 30wt%, and opaque white for 50wt%. It is thought that $ZrO_2 \cdot nH_2O$ was dispersed uniformly through the membrane. But, $ZrO_2 \cdot nH_2O$/S-PES composite membranes with over 60wt% $ZrO_2 \cdot nH_2O$ content could not be formed. In $ZrO_2 \cdot nH_2O$/S-PES composite membranes with high $ZrO_2 \cdot nH_2O$ content prepared by this method, $ZrO_2 \cdot nH_2O$ is aggregated in the membrane, and the membranes are brittle.

We examined the performance of the composite membranes with 10wt%, 30wt%, and 50wt% $ZrO_2 \cdot nH_2O$ content prepared by the precursor dispersion method.

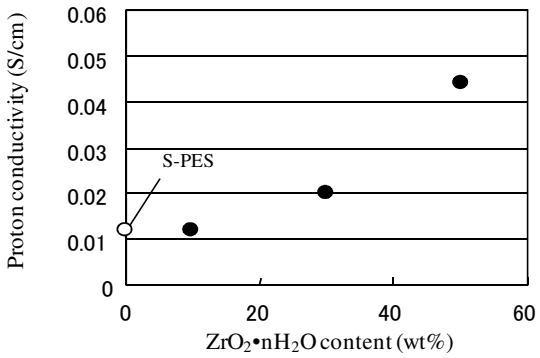

Figure 5. Proton conductivity of $ZrO_2 \cdot nH_2O$/S-PES (EW=1099) composite membranes as a function of $ZrO_2 \cdot nH_2O$ content (70 ºC)

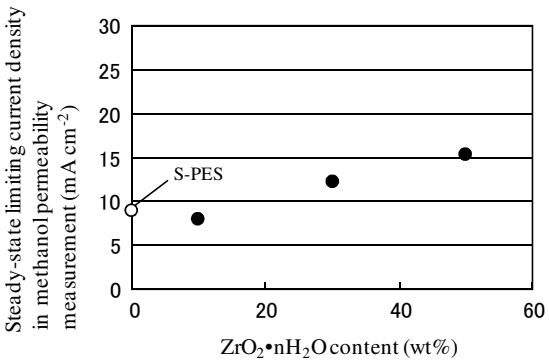

Figure 7. Methanol permeability of $ZrO_2 \cdot nH_2O$/S-PES (EW=1099) composite membranes as a function of $ZrO_2 \cdot nH_2O$ content (35 ºC)

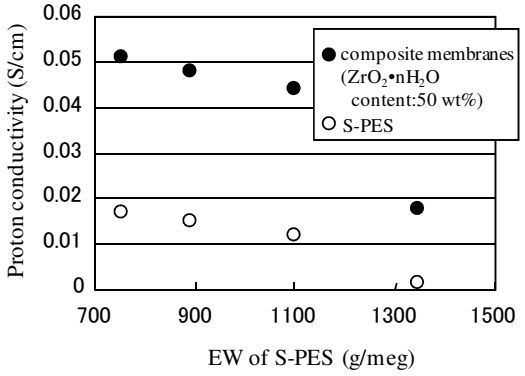

Figure 6. Proton conductivity of membranes as a function of the EW of S-PES (70 ºC)

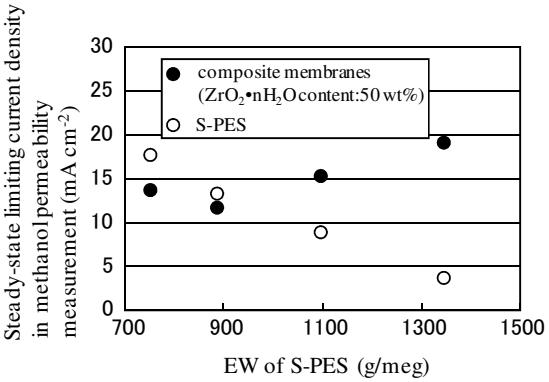

Figure 8. Methanol permeability of membranes as a function of the EW of S-PES (35 ºC)

3.2. Proton conductivity of membranes

Figure 5 shows the proton conductivity of $ZrO_2 \cdot nH_2O$/S-PES (EW=1099) composite membranes as a function of their $ZrO_2 \cdot nH_2O$ content. The white point ($ZrO_2 \cdot nH_2O$ content 0 wt%) shows the proton conductivity of an S-PES single polymer membrane. The proton conductivity of $ZrO_2 \cdot nH_2O$/S-PES composite membranes with 10 wt% $ZrO_2 \cdot nH_2O$ content was almost the same as that of an S-PES single polymer membrane. It is thought that the network of $ZrO_2 \cdot nH_2O$ in the membrane was not sufficiently formed in the case of low $ZrO_2 \cdot nH_2O$ content. Proton conductivity increased with an increase of $ZrO_2 \cdot nH_2O$ content. The proton conductivity of $ZrO_2 \cdot nH_2O$/S-PES composite membranes with 50wt% $ZrO_2 \cdot nH_2O$ content was about four times higher than that of the S-PES single polymer membrane.

Figure 6 shows the proton conductivity of $ZrO_2 \cdot nH_2O$/S-PES composite membranes ($ZrO_2 \cdot nH_2O$ content 50 wt%) as a function of the EW value of S-PES. For each EW value, the proton conductivity of the $ZrO_2 \cdot nH_2O$/S-PES composite membranes is superior to that of the S-PES single polymer membrane. Proton conductivity of the $ZrO_2 \cdot nH_2O$/S-PES composite membranes increased higher with lower EW values of S-PES.

3.3. Methanol permeability of membranes

Figure 7 shows the methanol permeability of $ZrO_2 \cdot nH_2O$/S-PES (EW=1099) composite membranes as a function of their $ZrO_2 \cdot nH_2O$ content. The vertical axis is the steady-state limiting current density in the methanol permeability measurement [22]. In this paper, we use the steady-state limiting current density as the flux rate of methanol permeability. The membranes have the same thickness, so high limiting current density means high methanol permeability. The steady-state limiting current density of Nafion112 was 83 mA cm^{-2}. The white point ($ZrO_2 \cdot nH_2O$ content 0wt%) shows the methanol permeability of S-PES single polymer membrane. The methanol permeability of $ZrO_2 \cdot nH_2O$/S-PES composite membranes with 10wt%, 30wt% and 50wt% $ZrO_2 \cdot nH_2O$ content was lower than that of Nafion112. The methanol permeability of $ZrO_2 \cdot nH_2O$/S-PES composite membranes increased with the increase of $ZrO_2 \cdot nH_2O$ content.

Figure 8 shows the methanol permeability of $ZrO_2 \cdot nH_2O$/S-PES composite membranes as a function of the EW value of S-PES. The methanol permeability of $ZrO_2 \cdot nH_2O$/S-PES composite membranes with EW values of 752, 850, 1099 and 1347 was lower than that of Nafion112. The methanol permeability of $ZrO_2 \cdot nH_2O$/S-PES composite membranes with low EW values was almost the same as that of S-PES, but it increased with increased EW values. The methanol permeability of $ZrO_2 \cdot nH_2O$/S-PES (EW=1099 and 1347) composite membranes was higher than that of S-PES.

One reason for increasing methanol permeability was that the

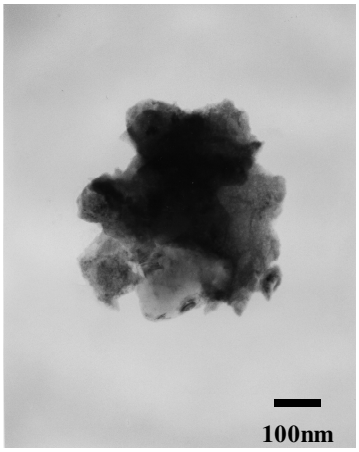

Figure 9. TEM image of $ZrO_2 \cdot nH_2O$/S-PES composite membrane

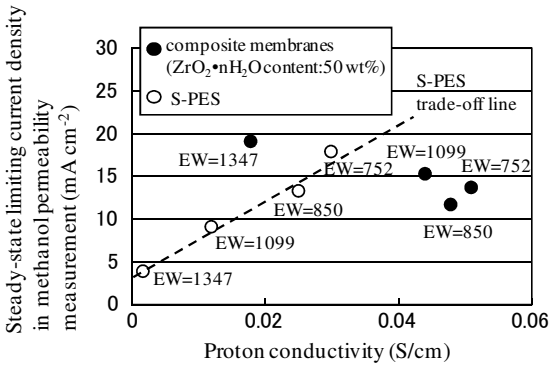

Figure 10. Summary of the proton conductivity and methanol permeability of the membranes

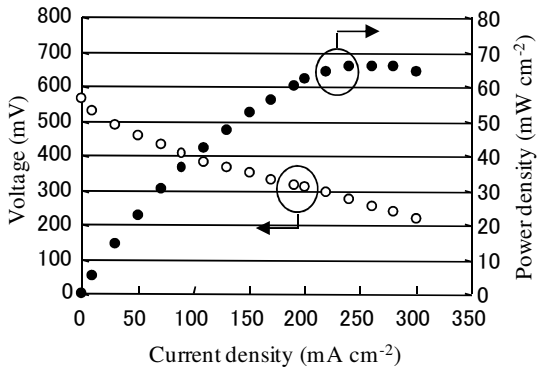

Figure 11. Initial I-V characteristic of an MEA consisting of $ZrO_2 \cdot nH_2O$/S-PES composite membrane (35 ºC)

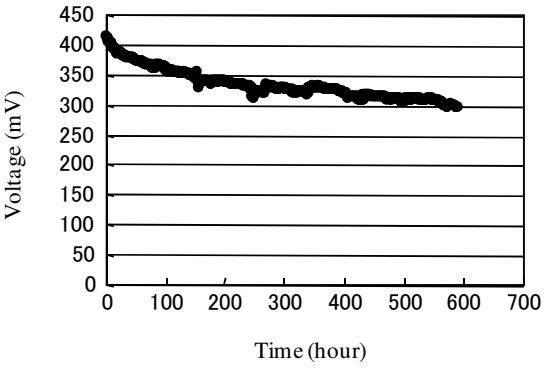

Figure 12. Performance stability of an MEA consisting of $ZrO_2 \cdot nH_2O$/S-PES composite membrane, investigated by galvanostatic operation at 50 mA cm^{-2} (35 ºC)

adhesion between $ZrO_2 \cdot nH_2O$ and S-PES was low. The addition of $ZrO_2 \cdot nH_2O$ alters the hydrophilic-hydrophobic balance inside the membranes because $ZrO_2 \cdot nH_2O$ shows hydrophilic features. The adhesion between $ZrO_2 \cdot nH_2O$ and S-PES might be lower with the increase of EW value because S-PES with high EW value was more hydrophobic. Thus, $ZrO_2 \cdot nH_2O$ repels S-PES, causing low adhesion between $ZrO_2 \cdot nH_2O$ and S-PES.

Another reason for the increasing methanol permeability might be that methanol permeated through the aggregated $ZrO_2 \cdot nH_2O$. Figure 9 shows TEM image of a $ZrO_2 \cdot nH_2O$/S-PES (EW=1099) composite membrane with 50wt% $ZrO_2 \cdot nH_2O$ content. Several hundred nanometer-scaled $ZrO_2 \cdot nH_2O$ were observed in the composite membrane. It was thought that a part of $ZrO_2 \cdot nH_2O$ was aggregated by the hundreds of nanometer size in the composite membranes. Therefore, there were spaces between aggregated $ZrO_2 \cdot nH_2O$ in the composite membrane.

3.4. Summary of proton conductivity and methanol permeability of the membranes

Figure 10 summarizes proton conductivity and methanol permeability of the membranes. The vertical axis is the steady-state limiting current density in the methanol permeability measurement, and the horizontal axis is the proton conductivity. The white points show the values for S-PES single polymer membranes. The broken line indicates the trade-off line of the S-PES single polymer membranes. In S-PES, protons are conducted through a sulfonic acid group while methanol also moves through the sulfonic acid group together with water, creating a trade-off between proton conductivity and methanol permeability. The black points show the values for $ZrO_2 \cdot nH_2O$/S-PES composite membranes prepared by the precursor dispersion method. The methanol permeability of $ZrO_2 \cdot nH_2O$/S-PES (EW=752 and 850) was almost the same as that of S-PES (EW=752 and 850) single polymer membranes, while the proton conductivity of the composite membrane improved. And, the methanol permeability of $ZrO_2 \cdot nH_2O$/S-PES (EW=1099) increased slightly compared with that of S-PES (EW=1099) single polymer membrane, while the proton conductivity of the composite membrane improved. These results mean that the trade-off relationship has been improved in the case of $ZrO_2 \cdot nH_2O$/S-PES (EW=752, 850 and 1099), compared with a S-PES single polymer membrane. On the other hand, the methanol permeability of $ZrO_2 \cdot nH_2O$/S-PES (EW=1347) increased significantly, compared with that of S-PES (EW=1347) single polymer membrane, which means that the trade-off relationship was not improved in the case of $ZrO_2 \cdot nH_2O$/S-PES (EW=1347).

3.5. I-V performance of MEA consisting of composite membrane

Figure 11 shows the initial I-V performance of an MEA consisting of a $ZrO_2 \cdot nH_2O$/S-PES (EW=850) composite membrane with 50wt% $ZrO_2 \cdot nH_2O$ content. We measured a maximum power density of 65 mW cm^{-2} at 260 mA cm^{-2}.

Figure 12 shows the performance stability of an MEA consisting of a composite membrane. The MEA was investigated by galvanostatic operation at 50 mA cm^{-2}. Voltage decayed from 420 mV to 320 mV in the first 250 hours of operation, then remained almost constant up to about 600 hours. The MEA consisting of the composite membrane shows good performance stability over time until about 600 hours. It was thought that $ZrO_2 \cdot nH_2O$ was not dissolved in the methanol solution and remained stable in the membrane for up to 600 hours.

4. CONCLUSIONS

We have prepared inorganic-organic membranes consisting of S-PES and $ZrO_2 \cdot nH_2O$. A preparation method using $ZrOCl_2 8H_2O$ as a precursor gave excellent uniformity. In the $ZrO_2 \cdot nH_2O$/S-PES composite membranes, the trade-off relationship between the proton conductivity and methanol permeability found in S-PES single polymer membranes was improved. The maximum power density of an MEA using the $ZrO_2 \cdot nH_2O$/S-PES composite membrane was 65 mW cm^{-2}. The MEA consisting of the composite membrane shows good performance stability up to 600 hours, investigated by galvanostatic operation.

REFERENCES

[1] S.R. Samms, S. Wasmus, R.F. Savinell, J. Electrochem. Soc., 143, 1498 (1996).
[2] T. Arimura, D. Ostrovskii, T. Okada, G. Xie, Solid State Ionics, 118, 1 (1999).
[3] J. Roziere, D.J. Jones, Annu. Rev. Mater. Res., 33, 503 (2003).
[4] S.C. Ball, Platinum Met. Rev., 49, 27 (2005).
[5] M. Rikukawa, K. Sanui, Prog.Polym. Sci., 25, 1463 (2000).
[6] T. Kobayashi, M. Rikukawa, K. Sanui, N. Ogata, Solid State Ionics, 106, 219 (1998).
[7] F. Lufrano, I. Gatto, P. Staiti, V. Antonucci, E. Passalacqua, Solid State Ionics, 145, 47 (2001).
[8] K. Miyatake, K. Oyaizu, E. Tsuchida, A.S. Hay, Macromolecules, 34, 2065 (2001).
[9] N. Miyake, J.S. Wainright, R.F. Savinell, J. Electorchem. Soc., 148, A905 (2001).
[10] B. Libby, W.H. Smyrl, E.L. Cussler, Electrochemical and Solid-State Letters, 4, A197 (2001).
[11] T. Mitsui, H. Morikawa, K. Kanamura, Electrochemistry, 70, 934 (2002).
[12] V.S. Silva, B. Ruffmann, H. Silva, Y.A. Gallego, A. Mendes, L.M. Madeira and S.P. Nunes, J. Power Sources, 140, 34 (2005).
[13] V.S. Silva, S. Weisshaar, R. Reissner, B. Ruffmann, S. Vetter, A. Mendes, L.M. Madeira and S. Nunes, J. Power Sources, 145, 485 (2005).
[14] H.W. Zhang, C.H. Du, Y.Y. Xu and B.K. Zhu, Polymers for Advanced Technologies, 18, 373 (2007).
[15] G. Alberti, M. Casciola, E. D'Alessandro and M. Pica, J. Mater. Chem., 14 1910 (2004).
[16] M.L. Hill, Y.S. Kim, B.R. Einsla and J.E. McGrath, J. Membrane Science, 283, 3972 (2006).
[17] H. Wu, Y. Wang and S. Wang, J. New Mater. Electrochem. Sys., 5, 251 (2002).
[18] O. Savadogo, J. Power Sources, 127, 135 (2004).
[19] O. Savadogo, J. New Mater. Electrochem. Sys., 1, 47 (1998).
[20] W.A. England, M.G. Cross, A. Hamnett, P.J. Wiseman and J.B. Goodenough, Solid State Ionics, 1, 231 (1980).
[21] F. Wang, M. Hickner, Q. Ji, W. Harrison, J. Mecham, T.A. Zawodzinski, J.E. McGrath, Macromol. Symp., 175, 387 (2001).
[22] X. Ren, T. E. Springer, A. Zawodzinski, S. Gottesfeld, J. Electrochem. Soc., 147, 466 (2000).